Journal of Materials Chemistry A

Accepted Manuscript

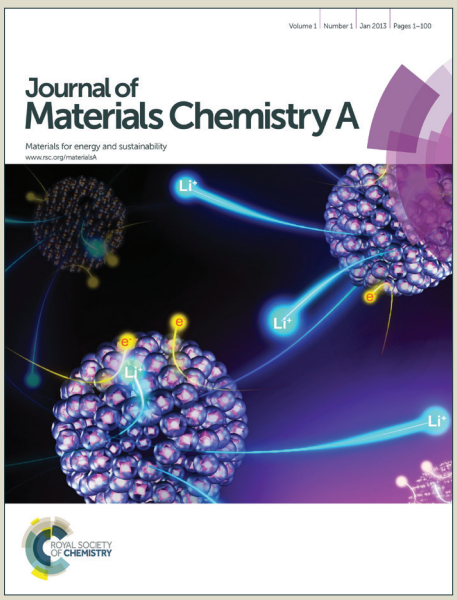

ROYAL SOCIETY OF CHEMISTRY

www.rsc.org/materialsA

Journal Name

RSCPublishing

ARTICLE

Taking steps forward in understanding the electrochemical behavior of $Na_2Ti_3O_7$

Cite this: DOI: 10.1039/x0xx00000x

Received 00th January 2015,
Accepted 00th January 2015

DOI: 10.1039/x0xx00000x

www.rsc.org/

J. Nava-Avendaño,[1] A. Morales-García,[2] A. Ponrouch,[1] G. Rousse,[3,4] C. Frontera,[1] P. Senguttuvan,[1,5] J.-M. Tarascon,[3,4] M. E. Arroyo-de Dompablo,[6*] M. Rosa Palacín[1*]

Na2Ti3O7 is an interesting negative electrode material for sodium ion batteries given its electrochemical capacity and low operation potential. Unfortunately its prospects of practical application are hindered by an unacceptable capacity fading upon cycling. In this work we combine experiments and DFT calculations to investigate the origin of such phenomenon. Different electrode technologies and different electrolytes have been targeted for electrochemical testing while the stability of Na2Ti3O7 and the fully reduced Na4Ti3O7 have been studied. The calculated elastic constants and vibrational modes support the mechanical and dynamical stability of the Na4Ti3O7 structure. In situ XRD measurements corroborate the reversibility of the insertion reaction as no structural damage is detected after 50 cycles. An intriguing reactivity of Na2Ti3O7 with the electrolyte upon storage is observed, which coupled to electrochemical measurements points at this being the main factor behind capacity fading.

Introduction

The development of room temperature sodium based batteries has emerged as a research priority in recent years, concomitant to prospects of batteries embracing larger scale energy storage applications coupled to sustainability concerns. Negative electrode materials such as nano-Sb[1], MoO_3[2], Fe_2O_3[3] or $NaTiO_2$[4] have been explored. Along this line, we recently reported on $Na_2Ti_3O_7$ which turned out to reversibly uptake 2 Na ions per formula unit (177 mAh/g) at an average potential of 0.3 V vs Na^+/Na,[5] which could potentially enable building high energy density Na-ion cells. Fundamental understanding of its redox mechanism and rationalization of the observed operation potential has been achieved combining experiments and first principles calculations.[6]

$Na_2Ti_3O_7$ crystallizes in the monoclinic system with $P2_1/m$ space group and cell parameters a= 8.5642(3) Å, b= 3.8012(1) Å and c= 9.1265(3) Å, and β= 101.598(2)º. Its crystal framework consists of TiO_6 octahedra linked by edges, forming zig-zag 3 x 2 x ∞ ribbons.[7] These ribbons are connected *via* vertices and stacked to form a layered structure. Sodium ions are located between the layers occupying two different crystallographic positions Na(1) and Na(2) (2e Wyckoff positions) that are 9- and 7-coordinated to oxygen atoms, respectively. In contrast, for $Na_4Ti_3O_7$ all the alkali ions would occupy octahedral sites and thus sodium ions migrated from their initial positions to more stable sites while the Ti-O framework remains mostly unaltered upon sodium insertion leading to a distorted rocksalt type structure with concomitant unit cell expansion of ca. 5%.[6]

Unfortunately the prospects of practical application for this compound have been to date hindered by the significant capacity fading generally observed upon cycling (~25% fading from first cycle over 10 to 25 cycles)[8,9,10,11,12] in samples prepared by diverse routes (solid state reaction or reverse microemulsion method) exhibiting particles with various morphologies and sizes and tested under different conditions. Carbon coating on the $Na_2Ti_3O_7$ particles to enhance its electronic conductivity has proved successful in improving the electrochemical performance of the material and allowed building a full Na-ion cell to prove the concept.[13] Yet, capacity of such cell based on the negative electrode falls to ca. 100 mAh/g after 30 cycles and self relaxation of $Na_4Ti_3O_7$ is proposed to cause self discharge which would be a critical bottleneck for application.

With the aim to get further insight on the reasons behind capacity fading and elucidate whether they are intrinsic to the material or technological in character, a detailed study was undertaken involving the electrochemical testing of $Na_2Ti_3O_7$ in different conditions. Such included *in situ* experiments aiming at detecting structural degradation after cycling and a detailed computational investigation of the mechanical and dynamical stability of the inserted phase $Na_4Ti_3O_7$.

Methodology

Experimental.- Pure $Na_2Ti_3O_7$ was prepared at 800 °C for 40h with intermediate regrinding from anatase TiO_2 (> 99.8%, Aldrich) and anhydrous Na_2CO_3 (>99.995%, Aldrich) with 10% excess of the latter with respect to stoichiometric amounts. The prepared $Na_2Ti_3O_7$ sample was found to be pure and consisted of irregularly shaped particles of 1-3 μm size (see S.I. in reference 5).

Electrochemical testing was carried out in two-electrode Swagelok® cells using sodium (99.9% Aldrich) as a counter electrode. Electrodes were prepared by three different protocols involving (i) simple powder mixtures of $Na_2Ti_3O_7$ with 30% of Super P carbon (TIMCAL) (ii) self standing electrodes were prepared using the Bellcore[14] technology from an acetone based slurry containing 70% of $Na_2Ti_3O_7$, 20 % Super P carbon, 10 % of polyvinylidene fluoride (PVDF) and dibutyl phthalate (DBP) as pore former, and which were further removed by washing the dry peeled off electrode with dietyl ether and (iii) tape casted electrodes on copper substrate from an n-methyl pyrrolidone (NMP) based slurry (65 % $Na_2Ti_3O_7$, 8 % PVDF and 27 % Super P carbon).[15] Two sheets of Whattman GF/d borosilicate glass fiber were used as a separator, soaked with the electrolyte which consisted of 1 M sodium salt (either NaTFSI, $NaClO_4$ or $NaPF_6$) in propylene carbonate (PC) alone or mixed with 50% ethylene carbonate. Typical electrode mass loading was 1 mg/cm^2 for tape casted electrode, 2 mg/cm^2 for Bellcore technology and 5 mg/cm2 for powder electrodes. All experiments were performed using a Bio-Logic VMP3 potentiostat.

Room temperature X-ray powder diffraction patterns were collected using a Bruker D8 laboratory diffractometer with CuKα radiation. Additional synchrotron powder diffraction patterns (SXRPD) were collected at ALBA synchrotron (λ=0.61988 Å) using a homemade Swagelok type cell using Be window to avoid exposure to air[16] and self standing electrodes containing and 1 M $NaClO_4$ in EC: PC as electrolyte and tested at C/8. SXRPD data were collected every 10 min (3 minutes acquisition time) all along the reduction process. For comparative purposes, the pattern of an identical electrode after 50 cycles was also measured. Rietveld refinements[17] were done using the FullProf program.[18]

About 100 mg of $Na_2Ti_3O_7$ sample were stored inside a glove box for 8 months in closed vials containing ca. 2 ml of common electrolytes and electrolyte solvents used for sodium-ion batteries a) propylene carbonate (PC), b) 50% ethylene carbonate: 50% propylene carbonate (EC: PC) c) 1 M $NaClO_4$ in EC: PC and c) 1 M $NaPF_6$ in EC: PC. The experiments were duplicated, with the second batch being kept at 60 ºC for the last two weeks. Once the storage tests were finished, the powders were recovered and washed once with dimethyl carbonate (DMC) that was left to evaporate at room temperature with subsequent drying at 60 ºC for 2 hours.

Computational.- First-principles calculations were performed using all-electron project augmented wave (PAW) method as implemented in the VASP code.[19] The strong on-site Coulomb interaction in the localized Ti 3d electrons was treated by the GGA+U approach (with U=3, 4 and 5 eV). The valence electrons are explicitly treated by plane-waves (PW) with a cutoff of 600 eV and Brillouin zone integrals are approximated using 4 x 8 x 4 k-points mesh for the monoclinic crystal. The crystal structures were fully relaxed and all calculations were carried out considering the spin polarized. More details can be found in reference 6. By means of the quasi-harmonic Debye model[20], it is possible to extrapolate the ab initio data to finite temperatures and evaluate the thermodynamic properties of the system. Under this approximation, the true phonon spectrum is replaced by a smooth function that depends on a single parameter: the Debye temperature, $\Theta_D(V)$. We have used this approximation to obtain preliminary thermodynamic information of the insertion reaction at finite temperature. GIBBS code[21], a thermodynamic package, allows us to automatically process the E(V) data obtained from DFT calculations and investigate the isothermal-isobaric thermodynamics of solids. In this work, thermal effects were computed using the Debye temperature calculated from the static bulk moduli and a Poison ratio of of 0.25 was used. The optimized $Na_4Ti_3O_7$ crystal structure was used to investigate its mechanical stability, we note that the crystal phase stability depends on the elastic constants (C_{ij}). The stresses for elastic constants are calculated on the relaxed structure using the tetrahedron method. The elastic constants of $Na_4Ti_3O_7$ are determined mainly based on the strains x = ± 0.015. Meanwhile the effect of U on elastic constant is also included. Additionally, we have studied the vibrational properties of $Na_4Ti_3O_7$, we calculated the normal vibrational modes of $Na_4Ti_3O_7$ in the γ-point using the Quantum Espresso code[22] under the density functional perturbation theory (DFPT). In summary, we have investigated the thermodynamic, mechanic, and dynamic properties to prove the stability of $Na_4Ti_3O_7$.

Results

a) Stability of $Na_4Ti_3O_7$.- The formation of $Na_4Ti_3O_7$ is expressed with the insertion reaction:

$$2\ Na + Na_2Ti_3O_7 \rightarrow Na_4Ti_3O_7 \qquad (1)$$

In a previous work we found this reaction to be thermodynamically favoured at 0 K (ΔG_r = - 72.23 kJ/mol), yielding a low average redox potential (0.36 V vs Na^+/Na). As discussed by Aydinol et al[23], in a lithium insertion reaction the entropy contribution to the free energy ($\Delta G_r = \Delta H_r - T\Delta S_r$) is of the order of 0.1 kJ/mol, which has a minor effect on the free energy/average voltage of the reaction. However, we decided to evaluate the thermodynamics of the insertion reaction (1) at room temperature, to exclude its implication in the capacity fading. We found that the free energy of the reaction increases in about 2 kJ/mol between 0 and 500 K (see Figure 1 in S.I.). This means a voltage variation below 0.02 V from 0K to RT, which confirms the negligible effect of temperature in the

thermodynamics of the insertion reaction. The estimated entropies at room temperature are 250 J/mol and 350 J/mol for $Na_2Ti_3O_7$ and $Na_4Ti_3O_7$, respectively. These values exclude entropic factors as a possible driving force for $Na_2Ti_3O_7$ and $Na_4Ti_3O_7$ to disorder.

Aiming to clarify whether the capacity fading of $Na_2Ti_3O_7$ electrode materials is related to a possible structural instability of the inserted phase, we have investigated the mechanical stability of $Na_4Ti_3O_7$ using first-principles calculations. The study of the mechanical staibility specifies the external stress under which the lattice is structurally unstable; stability requires that the whole set of elastic constant satisfies the Born-Huang criterion[24]. For a monoclinic crystal there are 13 independent elastic constants (C_{11}, C_{22}, C_{33}, C_{44}, C_{55}, C_{66}, C_{12}, C_{13}, C_{16}, C_{23}, C_{26}, C_{36}, and C_{45}). For our case, it is found that the calculated elastic constants (see Table I) obey this stability criteria (see supplemental information) and therefore the monoclinic $Na_4Ti_3O_7$ system is mechanically stable at the theoretical equilibrium volume. These results are independent of the used U parameter in the calculation; Table II lists selected calculated elastic constants for U = 0, 3, 4 and 5 eV.

Table 1.- Single-crystal elastic constants (C_{ij} in GPa) of $Na_4Ti_3O_7$ calculated at the theoretical equilibrium volume (U effect= 3 eV).

Cij		C_{12}	59.1
C_{11}	95.8	C_{13}	44.2
C_{22}	220.3	C_{16}	16.7
C_{33}	182.1	C_{23}	60.5
C_{44}	65.6	C_{26}	0.6
C_{55}	68.5	C_{36}	-5.9
C_{66}	62.8	C_{45}	2.9

Table 2.- Dependence of the calculated single-crystal elastic constants (C_{ij} in GPa) of $Na_4Ti_3O_7$ with the U parameter utilized in the calculation.

Cij	C11	C22	C33
U=0 eV	78.3	185.4	120.6
U=3 eV	95.8	220.3	182.1
U=4 eV	96.8	228.8	190.3
U=5 eV	96.6	235.4	195.1

Furthermore, for a crystal like $Na_4Ti_3O_7$, one can correlate the elastic constants values with the structural properties of the crystal. Since $Na_4Ti_3O_7$ is a monoclinic system, the elastic constant C_{11}, C_{22}, and C_{33} (95.8, 220.3 and 182.1 GPa, for U = 3 eV) can be directly related to the crystallographic *a*, *b*, and *c* axes respectively. The calculated values of these three constants follow the order $C_{22} > C_{33} > C_{11}$, which imply that the elastic constant C_{11} is the weakest for $Na_4Ti_3O_7$. This reveals the fact that a relative weakness of lattice interactions is present along the crystallographic *a* axis, which is parallel to the interlayer space. As previously discussed [6] the major variation upon alkali intercalation is observed for the *a* lattice parameter. As occurs in most layered materials, the distance between the layers decreases as more *A* ions are inserted, hence diminishing electrostatic repulsions. These sorts of interactions might confer some weakness to the material.

To investigate the dynamical stability of $Na_4Ti_3O_7$ the vibrational frequencies have been calculated at the γ-point. According to the symmetry and the number of atoms in the unit cell, 81 optical modes correspond to $Na_4Ti_3O_7$ (Gamma= $26B_u + 28A_g + 14B_g + 13A_u$). Their calculated intensity *vs* frecuency is shown in S.I. No imaginaries modes were found indicating the dynamical stability of this phase. In short, the computational results support the stability of the structural model proposed for the inserted $Na_4Ti_3O_7$. At this point, other hypotheses have to be considered to explain the poor capacity retention of $Na_2Ti_3O_7$.

b) Electrochemical testing under different conditions. Electrochemical tests performed using different electrode preparation protocols, and different electrolyte salts and solvents did not exhibit significant differences in terms of capacity retention and at least 25 % fading is always observed after 50 cycles. Nonetheless, some specific features were detected which were found to deserve a more detailed investigation, such as an additional redox feature appearing at ca. 1.3V in self standing electrodes, which were also those used in synchrotron radiation diffraction experiments.

The pattern of the pristine electrode (Figure 1a) does not correspond to $Na_2Ti_3O_7$ as expected but bears some similarities with that of $H_2Ti_3O_7$, which exhibits a structure related to that of $Na_2Ti_3O_7$ but with a shift of $[Ti_3O_7]^{2-}$ layers by b/2 along the b-direction and a C-centered cell (*C*2/*m* space group) with cell parameters *a = 16.02(1) Å, b= 3.746(1) Å, c = 9.1828 Å* and *β = 101.51 (1)°*.[25,8] Such findings can be tentatively attributed to a partial exchange between Na^+ and H^+ during the preparation of the electrode, due to the presence of traces of water in the acetone used. This could either result in a mixture of $Na_2Ti_3O_7$ and $H_2Ti_3O_7$ or to $Na_{2-x}H_xTi_3O_7$, which in view of the pattern seems more plausible (see Figure 3 in S.I). However, even if the electrode preparation process does induce a partial exchange between sodium ions and protons, this does not seem to be related to the capacity fading observed. Indeed, on one hand, exchange of protons with sodium ions from the electrolyte has been observed in tests using $H_2Ti_3O_7$ as electrode material in sodium cells as proved by *in situ* XRD measurements[8,26] and on the other, very similar capacity retention is observed for self standing and powdered electrodes. Thus, we believe that $Na_{2-x}H_xTi_3O_7$ gradually exchanges protons by sodium ions from the electrolyte and then exhibit the same electrochemical behavior as $Na_2Ti_3O_7$.

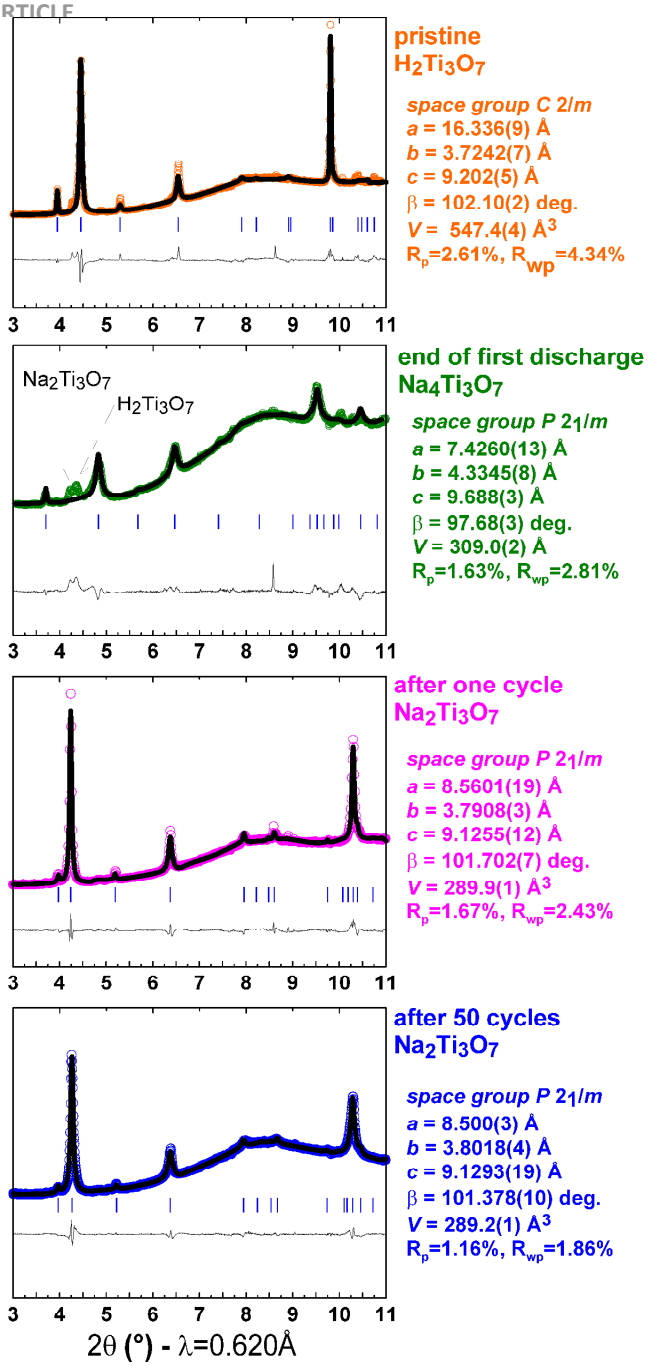

Figure 1.- Rietveld refinement of the SXRD patterns taken at a) the beginning of reduction ($H_2Ti_3O_7$), b) the end of reduction ($Na_4Ti_3O_7$), d) the end of reoxidation ($Na_2Ti_3O_7$) and e) after 50 cycles at the charged state.

The complete evolution of the SXRPD patterns collected during the full reduction as function of time is presented in Figure 2 (see also S.I. Figure4) . As seen in Figure 1a the initial SXRD pattern corresponds to the protonated $Na_{2-x}H_xTi_3O_7$ phase and can be fitted with the $H_2Ti_3O_7$ structure, with cell parameters (a= 16.336(9) Å, b= 3.7242(7) Å, c= 9.202(2) Å and β=102.10(2)º) very close to those reported for the pure phase, which make us conclude that the amount of sodium ions present in the electrode is almost negligible (x~1). As the reduction starts, changes in the intensity and position of the main two diffraction peaks are observed up to 1.25 V (t=3h) which can be attributed to the intercalation of sodium ions in the protonated phase. In addition, concomitant exchange of protons present in the sample with sodium ions from the electrolyte can also be expected, as previously reported for $Li_2Ti_3O_7$ when reduced in electrochemical cells using sodium containing electrolytes.[6] Moreover, the redox feature observed at 1.2V is in agreement with such hypothesis, as it has been previously observed when testing $H_2Ti_3O_7$ in sodium cells.[8,26] Further reduction proceeds with a pseudo plateau centered at ca. 0.6 V which does not seem to induce any change in the SXRPD patterns, in agreement with this phenomenon being attributed to the parasitic reaction of the electrolyte with SP carbon, as previously suggested. When reduction is pursued to potentials lower than 0.18 V (t= 25h), the evolution of a new set of diffraction peaks is observed that correspond to the reduced phase $Na_4Ti_3O_7$ which gradually grow to the expense of those corresponding to the pristine $Na_2Ti_3O_7$ phase. At the end of reduction, the SXRD patterns (Figure 1b) exhibit $Na_4Ti_3O_7$ as a major phase, with refined cell parameters a=7.4260(13), b=4.3345(8), c=9.688(3) and β=97.86(3)º, in good agreement with those predicted from DFT calculations. Unfortunately, some $H_2Ti_3O_7$ and $Na_2Ti_3O_7$ were still present in the electrode, which precluded the obtaining of further structural information from the data available.

Further on, the working electrode was reoxidized and an SXRPD pattern was taken at the end of oxidation (Figure 1c), which is typical of $Na_2Ti_3O_7$, with cell parameters in full agreement with expected values[5,6,7,9,10]: a= 8.5601(2) Å, b= 3.7908(3) Å, c= 9.1255(1) Å and β=101.70(2)º. Such results confirm that even if the initial phase in the electrode was $H_2Ti_3O_7$, proton exchange with sodium ions present in the electrolyte takes place so that the active phase present in the electrode during subsequent cycling is $Na_2Ti_3O_7$. This is in agreement with the very similar electrochemical behavior reported above for powdered and SSE electrodes prepared with $Na_2Ti_3O_7$, the latter found to contain $H_2Ti_3O_7$ instead. Figure 2c offers a graphic representation of the above results.

As seen in figures 1c and 1d, the SXRPD pattern on a self standing electrode after 50 cycles at C/15 is very similar to that of the electrode after one cycle with peaks becoming somewhat more lorentzian, which is in agreement with an enhancement in strains as typically observed for battery materials upon cycling. The refined cell parameters (see S.I.) (a=8.5001(3), b=3.8018(4), c=9.1293(19) and β=101.378(10)º) do not significantly differ from that of the electrode after one cycle which prompts us to conclude that capacity fading in $Na_2Ti_3O_7$ is not related to structural degradation of the phase upon cycling.

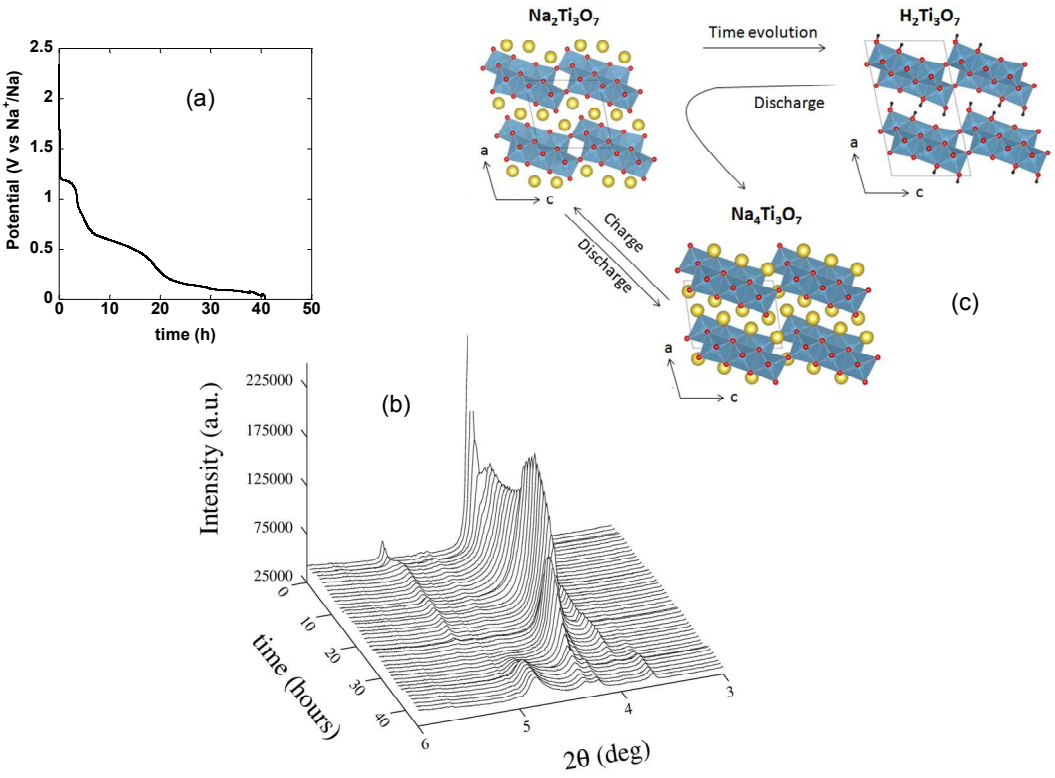

Figure 2.- a) Potential vs time profile for $Na_2Ti_3O_7$ SSE cycled vs Naº at C/8. b) 3-D plot showing the evolution of the SXRD patterns collected during electrochemical reduction as a function of time. c) Schematic representation of the observed processes upon time evolution and sodium intercalation

In view of such results tape casted electrodes were chosen for further electrochemical experiments, as the distribution of active material is expected to be much more homogeneous than those consisting of a simple mixture of powder with Super P carbon and at the same time no presence of H^+ in the structure is expected. The typical potential vs. capacity profile achieved is shown in Figure 3a with capacity gradually fading and also gradual shift of the curves to the right which is systematically observed and confirmed not to be related to any instrumental artifact clearly pointing at some degree of electrolyte reduction, most likely linked to the formation of a Solid Electrolyte Interphase (SEI). The cell polarization which can be observed at the end of reduction was found to slightly increase upon cycling (See inset in Figure 3b), which could be attributed to the formation of a non stable SEI layer. [27,28] This increase of cell polarization upon cycling is in agreement with Electrochemical Impedance Spectroscopy (EIS) measurements performed at the end of each oxidation cycle (See Figure 3d) which do clearly point at an enhanced charge transfer resistance upon cycling. Each EIS measurement was preceded by a 2 hours open circuit voltage period (see Figure 3c). It can be seen from Figure 3c that the initial OCV (before cycling) is stabilizing at ca. 2.35 V vs Na^+/Na while after cycling the OCV value is continuously decreasing upon cycling indicative of a modification of the electrode/electrolyte interface.

Such electrolyte reactivity may thus be at the origin of the observed capacity fading, which is in agreement with the capacity retention being higher at higher testing rate, with the lack of cell potential stabilization upon cell relaxation observed in previous studies. Such findings are also consistent with a very recent work published in the course of this study[29] reporting on a full solid- state sodium ion cell containing P_2- $Na_{2/3}[Fe_{1/2}Mn_{1/2}]O_2$ as positive electrode, a composite mixture of $Na_2Ti_3O_7/La_{0.8}Sr_{0.2}MnO_3$ as the negative electrode and Na-β''-Al_2O_3 solid electrolyte, which is tested at 350 ºC and exhibits a specific capacity of 152 mAh/g (referred to the positive electrode) which is retained (>90%) both at C/20 and 1C after 100 cycles. While it should be ascertained whether $La_{0.8}Sr_{0.2}MnO_3$ does in any way contribute to the redox behavior observed, such findings would thus confirm the intrinsic stability of the reduced phase even at high temperatures and also point at the parasitic reactions with liquid electrolytes being at the origin of the capacity fading observed.

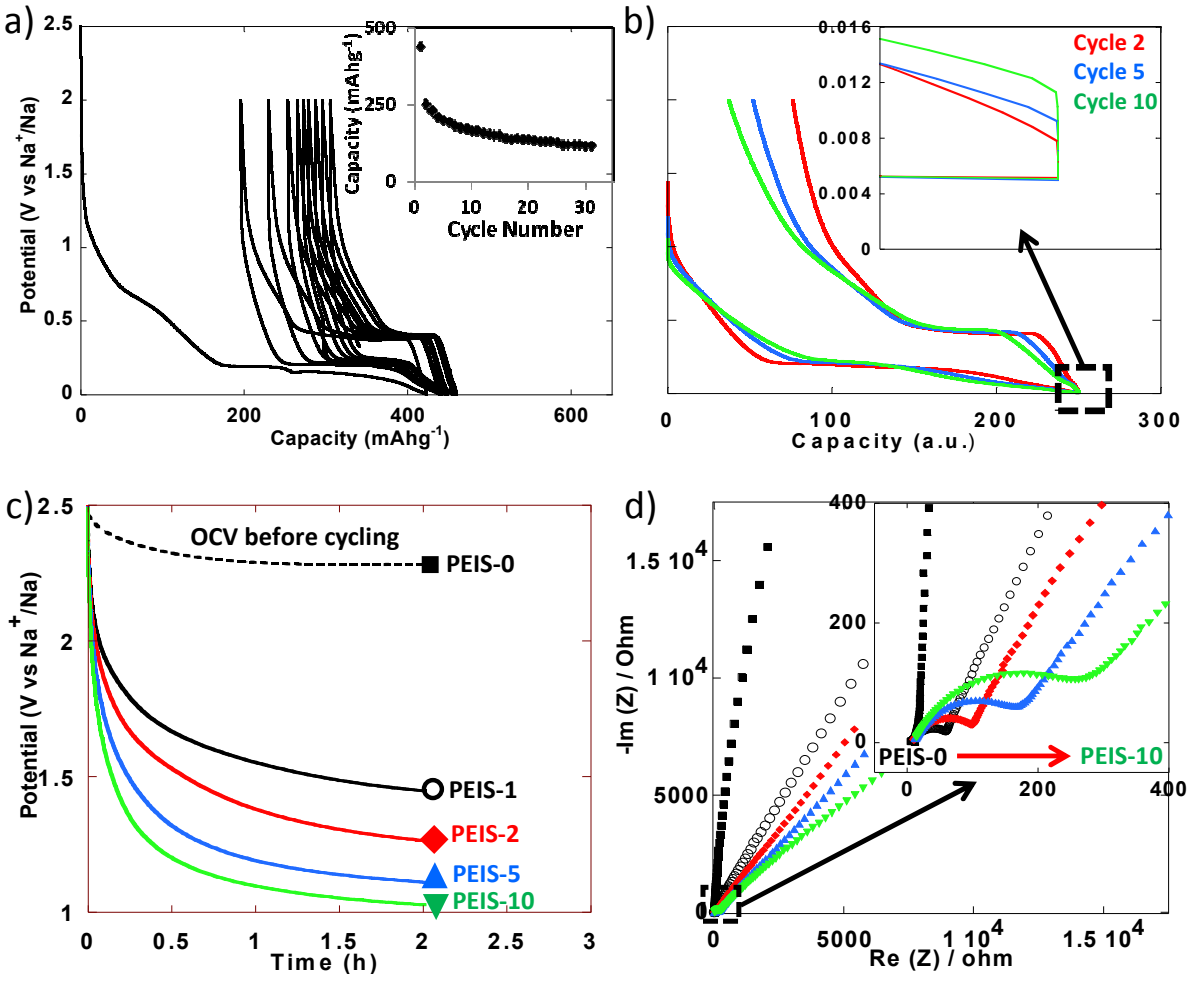

Figure 3.- Potential versus a) capacity and b) normalized capacity profiles for tape casted electrodes cycled in EC:PC based electrolyte (room temperature C/10). c) Open circuit voltage (OCV) recorded at the end of oxidation in b) before cycling (dashed curve) and after the first, second, fifth and tenth cycles (respectively, black, red, blue and green curves). d) Electrochemical impedance spectroscopy measurements performed after OCV period in c).

c) Stability of $Na_2Ti_3O_7$ in different electrolytes.

Given the above mentioned results and the surprising recently reports on the reactivity of $Li_4Ti_5O_{12}$ with LIB electrolyte solvents even in absence of any applied current,[30] we decided to check for the possibility of similar reactivity in the case of $Na_2Ti_3O_7$. The XRPD patterns of all the samples left to interact with the electrolytes at room temperature and 50 ºC depict a small decrease of the relative intensity of the diffraction peak at 2θ: 25.7º and the appearance of small intensity additional peaks which were found to correspond to $Na_2Ti_6O_{13}$ (2θ:11.85º, 14.06º and 24.49º). The nature of the salt or solvent used in the electrolyte does not seem to have a significant effect in such evolution, given that almost identical patterns are achieved for the samples stored in EC:PC and PC for both types of experiments. Selected XRPD patterns are shown in Figure 4, where the arrows denote peaks corresponding to $Na_2Ti_6O_{13}$.

Such transformation from $Na_2Ti_3O_7$ to $Na_2Ti_6O_{13}$ involves a condensation reaction and is unexpected at such low temperatures, as it has been previously been achieved only through thermal treatment of $Na_2Ti_3O_7$ at temperatures ranging from 300 to 800 ºC.[31,32] The mechanism of such reaction at room temperature is currently unclear, but such unexpected results prove that there is interaction of $Na_2Ti_3O_7$ with the electrolyte and make us suspect that some surface reactivity may also exist between the electrolyte and the reduced $Na_4Ti_3O_7$ which may be even more reactive, since it contains titanium in mixed oxidation state. Thus, these preliminary results point at degradation of the active material due to reactivity with the electrolyte as one of the plausible causes contributing to capacity fading.

Conclusions

Optimizing the electrochemical performance of $Na_2Ti_3O_7$ requires the elucidation of the origin for the poor capacity retention observed by different authors. The presented computational results indicate that the inserted $Na_4Ti_3O_7$ phase is mechanically and dynamically stable, discarding the instability of $Na_4Ti_3O_7$ as a key issue in the capacity fading. The reversibility of the insertion reaction has been certified; our

in-situ XRD reveal that the initial $Na_2Ti_3O_7$ is recovered after 50 cycles. We conclude that $Na_2Ti_3O_7$ and its sodiated phase $Na_4Ti_3O_7$ are structurally stable, and the insertion reaction fully reversible.

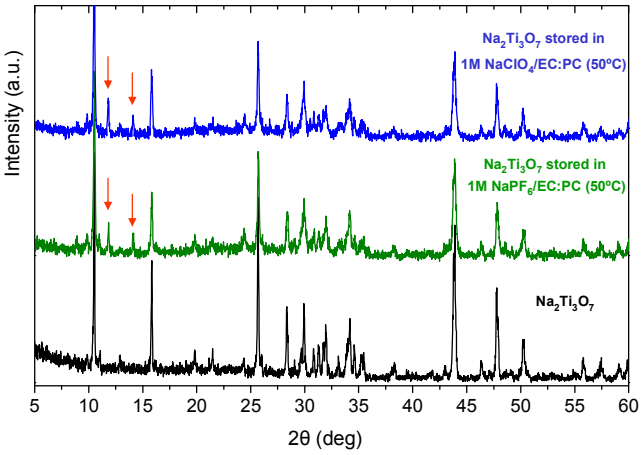

Figure 4. Evolution of XRPD patterns of $Na_2Ti_3O_7$ after 8 months stored in different electrolytes/electrolyte solvents.

However, we have observed an enhanced reactivity of $Na_2Ti_3O_7$ with liquid electrolytes. Such reactivity occurs even without an applied field, by simply storing the fresh $Na_2Ti_3O_7$ material in the electrolyte. Similar reactivity is expected for the inserted phase. This reactivity concomitant with the degradation of the SEI is proposed as the origin of the poor capacity retention. Further efforts should be pursued in order to fully confirm the above mentioned assumptions and fully assess the practical prospects of $Na_2Ti_3O_7$ as negative electrode material for sodium ion batteries.

Acknowledgements

We thank Dr. Maria Alfredsson and ALISTORE-ERI members for fruitful discussions and acknowledge Ministerio de Ciencia e Innovación for grants MAT2014-53500-R, CSD2007-00045 (MALTA-Consolider) and CTQ2012-28599-C02. We are grateful to Alba synchrotron for beamtime allocation (proposal 2013100585) and to Dr. François Fauth for his assistance during data collection. M.E. Arroyo acknowledges access to computational resources from Universidad de Oviedo (MALTA cluster) and the Spanish's national high performance computer service (I2 Basque Centre).

Notes and references

[1] Institut de Ciència de Materials de Barcelona (ICMAB-CSIC) Campus UAB, E-08193 Bellaterra, Catalonia (Spain).
[2] Department of Physical and Macromolecular Chemistry, Faculty of Science, Charles University in Prague, Hlavova 2030, Prague 2, 128 43, Prague (Czech Republic).
[3] FRE 3677 "Chimie du Solide et Energie", Collège de France, 11 Place Marcelin Berthelot, 75231 Paris Cedex 05 (France).
[4] Sorbonne Universités - UPMC Univ Paris 06, 4 Place Jussieu, F-75005 Paris (France).
[5] Laboratoire de Réactivité et Chimie des Solides, UPJV, CNRS UMR6007, 33 rue Saint Leu 80039 Amiens (France).
[6] Departamento de Química Inorgánica, Universidad Complutense de Madrid, 28040 Madrid (Spain).
*Corresponding authors: e.arroyo@quim.ucm.es ; rosa.palacin@icmab.es

References

1 X. Zhou, Y. Zhong, M. Yang, M. Hu, J. Weia and Z. Zhou, Chem. Commun., 2014, 50, 12888
2 S. Hariharan, K. Saravanan, P. Balaya, Electrochem. Comm. 2013, 31, 5
3 M. Valvo, F. Lindgren, U. Lafont, F. Björefors and K. Edström, J. Power Sources, 2014, 245, 967
4 D. Wu, X. Li, B. Xu, N. Twu, L. Liu and G. Ceder, Energy Environ. Sci., 2015, 8, 195
5 P. Senguttuvan, G. Rousse, V. Seznec, J.M. Tarascon, M.R. Palacin. Chem. Mater. 2011, 23, 4109.
6 G. Rousse, M.E. Arroyo-de Dompablo, P. Senguttuvan, A. Ponrouch, J.M. Tarascon, M.R. Palacín. Chem. Mater. 2013, 25, 4946.
7 S. Andersson, A.D Wadsley, A.D. Acta Cryst. 1961, 14, 1245.
8 P. Senguttuvan. PhD Thesis. Universite de Picardie. 2013
9 A. Rudola, K. Saravanan, C.W. Mason, P. Balaya. J. Mater. Chem.A 2013, 1, 2653.
10 H. Pan, X. Lu, X. Yu, Y.S. Hu, H. Lo, X.Q. Yang, L. Chen. Adv. Energy Mater.2013, 3, 1186.
11 W. Wang, C. Yu, Y. Liu, J. Hou, H. Zhu, S. Jiao. RSC Adv. 2013, 3, 1041.
12 W. Zhou, J. Li, Q. Deng, J. Xue, X. Dai, A. Zhou, J. Li. Solid State Ionics 2014, 262, 192.
13 J. Xu, C. Ma, M. Balasubramanian, Y.S. Meng. Chem. Commun. 2014, 50, 14029.
14 J.M. Tarascon, A.S. Gozdz, C. Schmutz, F. Shokoohi, P.C. Warren. Solid State Ionics 1996, 86, 49.
15 A. Ponrouch, M.R. Palacin, J. Power Sources 2011, 196, 9682.
16 M. Morcrette, Y. Chabre, G. Vaughan, G. Amatucci, J.B. Leriche, S. Patoux, C. Masquelier, J.M. Tarascon, Electr. Acta 2002, 47, 3137.
17 H.M. Rietveld, J. Appl. Crystallogr. 1969, 2, 65.
18 J. Rodríguez-Carvajal, . Phys. B Condens. Matter 1993, 192, 55.
19 G. Kresse, J. Furthmüller, J. Comput. Mater. Sci. 1996, 6, 15.
20 Y. Zhang, X. Ke, C. Chen, J. Yang, P. Kent, Phys. Rev. B 2009, 80, 024304.
21 M. Blanco, E. Francisco, V. Luaña, Computer Physics Comm. 2004, 158, 57.
22 P. Giannozzi, et al. J. Phys.:Condens. Matter, 2009, 21, 395502.
23 K.M. Aydinol, A. F. Kohan, G. Ceder, K. Cho, J. Joannopoulos, Phys. Rev. B 1997, 56, 1354
24 M. Born and K. Huang, in Dynamical Theory of Crystal Lattices; Oxford University Press: Oxford, 1998.
25 T.P. Feist, P.K. Davies, J. Solid State Chem. 1992, 101, 275.
26 A. Eguía-Barrio, E. Castillo-Martínez, M. Zarrabeitia, M.A: Muñoz-Márquez , M. Casas-Cabanas M, and T. Rojo, Phys Chem Chem Phys. 2015, 17, 6988.
27 A. Ponrouch, E. Marchante, M. courty, J.M. Tarascon, M.R. Palacín. Energy Environ. Sci. 2012, 5, 8572.

28 A. Ponrouch, R. dedryvere, D. Monti, A.E. Demet, J.M. Ateba Mba, L. Croguennec, C. Masquelier, P. Johansson, M. R. Palacin, Energy Environ. Sci. 2013, 6, 2361.
29 T. Wei, Y. Gong, X. Zhao, K. Huang. Adv. Funct. Mater., 2014 24 5380.
30 Y.B. He, B. Li, M. Liu, C. Zhang, W. Lu, C. Yang, J. Li, H. Du, B. Zhang, Q.H. Yang, J.K. Kim, F. Kang. Sci. Rep, 2012, 2 913.
31 S. Papp, L. Korosi, V. Meynen, P. Cool, E.F. Vansant, I. Dekany. J. Solid State Chem. 2005, 178, 1614.
32 H. Liu, D. Yang, Z. Zheng, X. Ke, E. Waclawik, H. Zhu, R.L. Frost. J. Raman Spectrosc. , 2010, 41, 1331.

TOC for Manuscript ID: TA-ART-07-2015-005174
TITLE: Taking steps forward in understanding the electrochemical behavior of Na2Ti3O7

A combination of experiments and calculations allows grasping more information on the capacity fading upon cycling of $Na_2Ti_3O_7$ electrode material in Na batteries